

Conformation of (Z)-3-Carboxymethyl-[(2E)-2-methyl-3-phenylpropenylidene]-rhodanine (Epalrestat), a Potent Aldose Reductase Inhibitor: X-Ray Crystallographic, Energy Calculational, and Nuclear Magnetic Resonance Studies

Toshimasa Ishida,* Yasuko In, Masatoshi Inoue, and Chiaki Tanaka
Osaka University of Pharmaceutical Sciences, 2-10-65 Kawai, Matsubara, Osaka 580, Japan
Nobuyuki Hamanaka*
ONO Pharmaceutical Co. Ltd., 3-1-1 Sakurai, Shimamoto, Mishima, Osaka 618, Japan

In order to examine the conformational characteristics of aldose reductase inhibitors, the conformational analysis of epalrestat (ONO-2235) has been carried out by X-ray crystallographic, energy calculational, and nuclear magnetic resonance methods. The chemical structure which had previously been proposed for epalrestat has been revised by the X-ray single-crystal analysis. The extremely planar conformation observed in the crystal structure is shown to be energetically the most stable form and is the predominant form in solution. The characteristic conformation is discussed with respect to the aldose reductase inhibitory activity.

The incidence of diabetic complications, *e.g.* diabetic neuropathy, nephropathy, retinopathy, and cataract, has become more critical in recent years. It is believed that aldose reductase (AR, EC 1.1.1.21) plays a physiologically significant role in the initiation of such diabetic complications.¹⁻⁴ This enzyme, one of the NADPH-dependent aldo-keto reductases, is involved in the sorbitol pathway and is an important regulator of mammalian glucose metabolism.⁵ For diabetes, excessive sorbitol production from glucose by AR is thought to cause cellular damage as a result of osmotic imbalance,^{2,6} which is linked to the development of diabetic complications. Although the exact mechanism of the polyol metabolic pathway is still unknown, however, increased importance has been placed on the development of potent aldose reductase inhibitors (ARIs), which are viewed as a means to reduce diabetic complications. Numerous compounds have been screened for potential activity as ARIs, and some representatives are listed in Table 1; their inhibitory activities for human placenta aldose reductase (HPAR) and rat or rabbit lens aldose reductase (RLAR or RaLAR) are also given.⁷⁻¹³

In order to design effectively compounds exhibiting high AR inhibitory activity, it is of special importance to know the key atoms and their spatial disposition necessary for inhibitory activity. To achieve this end, structural elucidation of an AR-ARI complex crystal by X-ray diffraction could be most straightforward. Under the present circumstances where such crystal analyses have not yet been completed,^{14,15} however, we consider that a possible alternative method would be to compare the stable conformations of potent ARIs and to extract their common spatial features.

As part of a series of structural studies on the molecular conformation-activity relationships of ARIs,¹⁶ we deal here with the molecular conformation of epalrestat studied by X-ray crystallographic, energy calculational, and NMR methods, and we also consider the conformational characteristics which are closely related with inhibitory activity.

Experimental

Materials.—Epalrestat was obtained as the sole product by condensation of rhodanin-*N*-acetic acid and α -methylcinnamaldehyde in acetic acid in the presence of sodium acetate.¹⁷ After

many attempts to obtain single crystals, yellow plates of a suitable size for X-ray study were crystallized from ethanol solution by slow evaporation at room temperature.

X-Ray Crystal Analysis.—The crystals are very fragile and rapidly become opaque on evaporation of solvent molecules of crystallization. For the X-ray study, therefore, a single crystal with dimensions *ca.* 0.3 × 0.2 × 0.1 mm was sealed in a glass capillary in the presence of some mother liquor. Cell parameters were obtained from a least-squares fit of the setting angles of 25 reflections measured on a Rigaku AFC-5 diffractometer with graphite-monochromated Cu-K α radiation (λ 1.5405 Å).

Crystal data. C₁₅H₁₃NO₃S₂·C₂H₅OH, *M* = 365.46, triclinic, *P* $\bar{1}$, *a* = 14.968(3), *b* = 8.528(2), *c* = 8.403(2) Å, α = 119.80(2), β = 100.82(3), γ = 75.09(2)°, *V* = 897.3(4) Å³, *D_m* = 1.341(3), *D_x* = 1.353 g cm⁻³, *Z* = 2, μ (Cu-K α) = 28.17 cm⁻¹, *F*(000) = 384.

X-Ray diffraction intensities with $2\theta < 130^\circ$ were collected with the same diffractometer employed in the ω - 2θ scan technique with a scan speed of 3° min⁻¹. Since the reflection peaks were rather broad and shapeless because of the poor crystal quality, the relatively wide range of (1.7 + 0.15 tan θ)° was scanned for each reflection. Four standard reflections, measured at every 100 reflection intervals, showed no significant structural deterioration during the data collection. The measured intensities were corrected for Lorentz and polarization factors. Absorption correction was applied based on the intensity variation of the ϕ scan of a reflection near to $\chi = 90.0^\circ$. Out of the measured 3 052 independent intensities, 2 196 having $F_o^2 \geq 3\sigma(F_o)^2$ were considered as observed and were used for the structure determination and refinement, where $\sigma(F_o)^2$ is the standard deviation based on counting statistics.

The structure was solved by direct methods with the MULTAN78 program.¹⁸ The co-ordinates obtained for the non-hydrogen atoms were refined by full-matrix least-squares with isotropic thermal parameters, and then by the block-diagonal least-squares method with anisotropic thermal parameters. The ideal positions for the hydrogen atoms, except for those of solvent ethanol, were calculated, and some were also verified on a difference Fourier map, and then included in the further refinement with overall isotropic thermal parameters (6.0 Å²). The function minimized was $\sum w(|F_o| - |F_c|)^2$, where

Table 1. Chemical structures of some representative ARIs with inhibitory activities for AR enzymes.

Name	Chemical structure	Inhibitory activity IC_{50} ($\mu\text{mol dm}^{-3}$)	
		HPAR	RLAR
Epalrestat		0.026	0.01
Sorbinil		0.68	0.07
Alconil			0.024
Alrestatin		6.5	1.5
Tolrestat			0.011
Statil		0.15	0.016
4-Isopropyl-BPOC			0.35 (RaLAR)

$|F_o|$ and $|F_c|$ are the observed and calculated structure amplitudes, respectively. The weighting scheme used for the final refinement was as follows: $w = 1.0/[\sigma(F_o)^2 + 0.05077|F_o| - 0.00063|F_o|^2]$. Discrepancy indexes R ($= \Sigma||F_o| - |F_c||/\Sigma|F_o|$) and R_w ($= [\Sigma w(|F_o| - |F_c|)^2/\Sigma w|F_o|^2]^{1/2}$) were 0.072 and 0.052, respectively, and S ($= [\Sigma w(|F_o| - |F_c|)^2/(M - N)]^{1/2}$, where M = number of observed reflections, N = number of variables used for refinement) was 1.154. Final co-ordinates for non-hydrogen atoms are given in Table 2.* For all crystallographic computations, the UNICS programs¹⁹ were used, and atomic scattering factors were cited from ref. 20.

Conformational Energy Calculations.—The conformational energy of epalrestat was calculated by the molecular mechanics method [CHEMLAB-II version²¹]. The energy functions included in the calculations were steric (Lennard-Jones potential), electrostatic (Coulombic), and torsional energies as

* Supplementary data (see section 5.6.3 of Instructions for Authors, in the January issue). Anisotropic temperature factors of non-hydrogen atoms and the hydrogen-atom co-ordinates have been deposited at the Cambridge Crystallographic Data Centre.

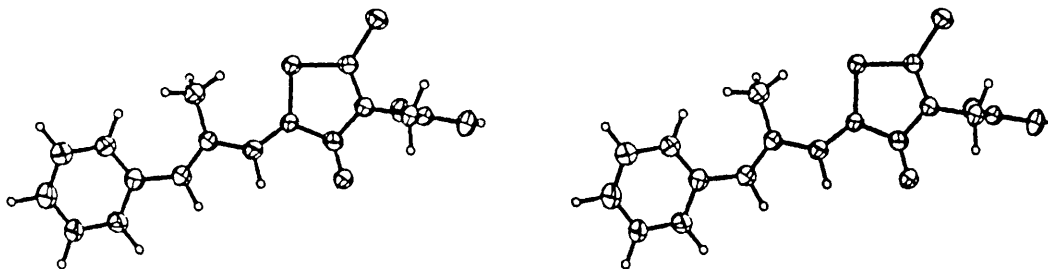


Figure 1. Stereoscopic drawing of epalrestat observed in the crystal structure.

Table 2. Atomic co-ordinates of non-hydrogen atoms of epalrestat, with e.s.d.s in parentheses.

Atom	x	y	z
C(1)	0.871 6(3)	-0.094 6(6)	0.311 5(6)
O(1)	0.847 7(2)	-0.154 2(5)	0.392 1(4)
O(1')	0.956 7(2)	-0.127 8(5)	0.262 4(5)
C(2)	0.808 5(3)	0.037 7(6)	0.246 3(6)
N(2)	0.715 6(2)	0.077 2(5)	0.291 8(4)
C(3)	0.653 4(3)	-0.035 9(6)	0.178 3(6)
S(3)	0.674 48(9)	-0.226 9(2)	-0.016 4(2)
S(4)	0.546 43(8)	0.050 3(2)	0.268 5(2)
C(4)	0.586 2(3)	0.236 5(6)	0.463 0(6)
C(5)	0.683 1(3)	0.230 8(6)	0.453 1(6)
O(5)	0.730 9(2)	0.336 6(4)	0.561 9(4)
C(6)	0.539 7(3)	0.370 8(6)	0.619 3(6)
C(7)	0.446 4(3)	0.410 1(6)	0.660 5(6)
C(8)	0.424 4(3)	0.552 2(6)	0.825 2(6)
C(9)	0.379 8(3)	0.292 3(8)	0.516 8(7)
C(10)	0.337 1(3)	0.634 6(7)	0.916 5(7)
C(11)	0.335 5(3)	0.798 7(7)	1.080 9(6)
C(11')	0.260 1(3)	0.559 2(7)	0.864 7(7)
C(12)	0.257 3(3)	0.891 3(7)	1.178 7(7)
C(12')	0.182 9(4)	0.642 8(8)	0.967 1(7)
C(13)	0.181 6(4)	0.812 0(8)	1.117 9(8)
O(1)E ^a	0.917 4(2)	0.357 2(6)	0.659 8(6)
C(2)E	0.942(1)	0.533(4)	0.737(8)
C(3)E	0.871(1)	0.706(2)	0.817(2)

^a The suffix letter E represents ethanol molecule.

calculated from equations (1)–(3), where r_{ij} in equations (1) and

$$E_{steric} = \sum_i \sum_j (-A_{ij} r_{ij}^{-6} + B_{ij} r_{ij}^{-12}) \quad (1)$$

$$E_{elec} = \sum_i \sum_j 332.0 \cdot Q_i \cdot Q_j \cdot r_{ij}^{-\epsilon} \quad (2)$$

$$E_{tor} = A[B + C \cos^M(N\theta - \phi)] + D[1 - \cos(E\theta - \psi)] \quad (3)$$

(2) is the distance (in Å) between atoms i and j . The atomic net charge on atom i (Q_i) in equation (2) was calculated by the quantum chemical MNDO method,²² and the dielectric constant (ϵ) was taken as 4.0, close to the experimental values for biomolecules in polar media. The A, B, C, D, E, M, N, θ , ϕ , and ψ symbols in equations (1) and (3) are constants associated with a particular type of bond.²³ All calculations of equations (1)–(3) were performed with the supplied data set.²¹ The atomic co-ordinates obtained by X-ray analysis were used for the calculations. Various conformations of epalrestat were built up by the rotations of torsion angles ω_1 [C(4)–C(6)–C(7)–C(8)] and ω_2 [C(7)–C(8)–C(10)–C(11)] (see Table 1); these torsion angles were rotated in 10° increments from 0 to 360°, where the starting, eclipsed conformation was 0°. The rotation about the C(2)–N(2) bond was fixed at the value observed in the crystal

Table 3. Bond lengths (Å) and angles (°) for epalrestat, with e.s.d.s in parentheses.

C(1)–O(1)	1.171(6)	C(6)–C(7)	1.416(7)
C(1)–O(1')	1.329(6)	C(7)–C(8)	1.339(7)
C(1)–C(2)	1.529(7)	C(7)–C(9)	1.523(7)
C(2)–N(2)	1.423(6)	C(8)–C(10)	1.469(7)
N(2)–C(3)	1.385(6)	C(10)–C(11)	1.393(7)
N(2)–C(5)	1.394(6)	C(10)–C(11')	1.359(8)
C(3)–S(3)	1.646(5)	C(11)–C(12)	1.382(8)
C(3)–S(4)	1.724(5)	C(11')–C(12')	1.387(8)
S(4)–C(4)	1.757(5)	C(12)–C(13)	1.356(8)
C(4)–C(5)	1.455(7)	C(12')–C(13)	1.366(9)
C(4)–C(6)	1.400(7)	O(1)E–C(2)E	1.42(4)
C(5)–O(5)	1.196(6)	C(2)E–C(3)E	1.49(5)
O(1)–C(1)–O(1')	126.7(3)	C(4)–C(5)–O(5)	127.8(3)
O(1)–C(1)–C(2)	124.8(3)	C(4)–C(6)–C(7)	131.5(3)
O(1')–C(1)–C(2)	108.5(3)	C(6)–C(7)–C(8)	115.9(3)
C(1)–C(2)–N(2)	111.6(3)	C(6)–C(7)–C(9)	118.7(3)
C(2)–N(2)–C(3)	121.5(3)	C(8)–C(7)–C(9)	125.5(3)
C(2)–N(2)–C(5)	121.5(3)	C(7)–C(8)–C(10)	132.2(3)
C(3)–N(2)–C(5)	117.0(3)	C(8)–C(10)–C(11)	116.9(3)
N(2)–C(3)–S(3)	126.7(2)	C(8)–C(10)–C(11')	126.4(3)
N(2)–C(3)–S(4)	110.5(2)	C(11)–C(10)–C(11')	116.5(3)
S(3)–C(3)–S(4)	122.8(1)	C(10)–C(11)–C(12)	122.5(3)
C(3)–S(4)–C(4)	92.3(2)	C(10)–C(11)–C(12')	122.0(4)
S(4)–C(4)–C(5)	110.7(2)	C(11)–C(12)–C(13)	118.2(4)
S(4)–C(4)–C(6)	128.8(2)	C(11')–C(12)–C(13)	119.1(4)
C(5)–C(4)–C(6)	120.3(3)	C(12)–C(13)–C(12')	121.1(4)
N(2)–C(5)–C(4)	109.5(3)	O(1)E–C(2)E–C(3)E	121.1(1)
N(2)–C(5)–O(5)	122.7(3)		

Table 4. Selected torsion angles (°) for epalrestat, with e.s.d.s in parentheses.

O(1)–C(1)–C(2)–N(2)	-1.4(4)
O(1')–C(1)–C(2)–N(2)	179.1(4)
C(1)–C(2)–N(2)–C(3)	-85.8(4)
C(1)–C(2)–N(2)–C(5)	93.8(4)
S(4)–C(4)–C(6)–C(7)	-7.6(4)
C(5)–C(4)–C(6)–C(7)	177.4(7)
C(4)–C(6)–C(7)–C(8)	-179.3(6)
C(4)–C(6)–C(7)–C(9)	-0.2(4)
C(6)–C(7)–C(8)–C(10)	179.9(7)
C(9)–C(7)–C(8)–C(10)	0.8(6)
C(7)–C(8)–C(10)–C(11)	-171.8(6)
C(7)–C(8)–C(10)–C(11')	13.9(5)

structure, because this orientation could be the energetically most stable one (discussed later).

The numerical calculations were performed on a MicroVAX II computer at the Computation Center, Osaka University of Pharmaceutical Sciences.

NMR Measurements.—The ¹H NMR measurements were carried out at a low concentration (ca. 1 mg ml⁻¹) in [2H₆]-

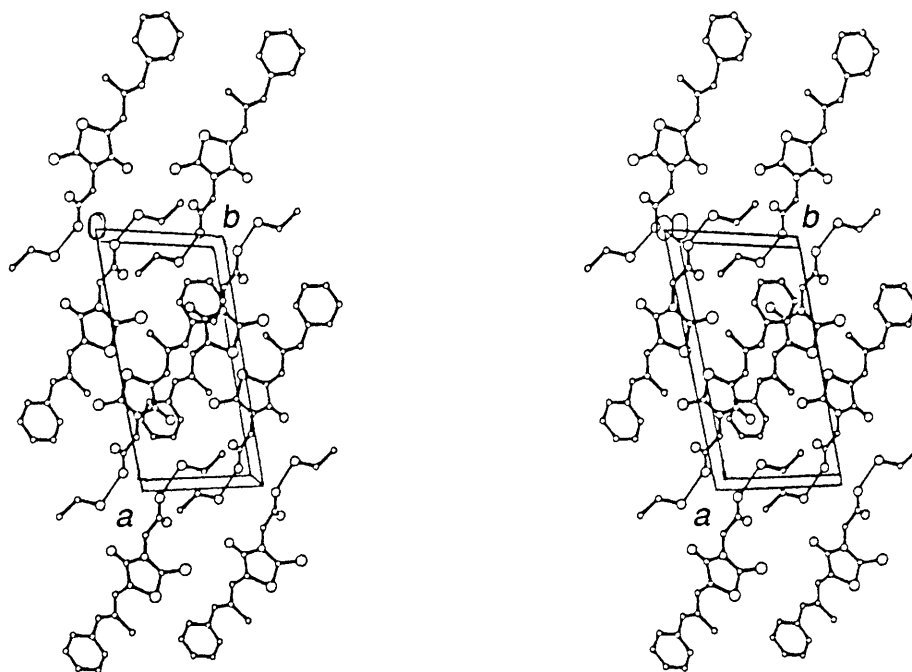


Figure 2. Stereoscopic view of epalrestat crystal viewed along the *c*-axis. The thin lines represent possible hydrogen bonds.

Table 5. Optimal planes and deviations (Å) of individual atoms of epalrestat, and dihedral angles (°).

(1) Equations of the best planes expressed by $m_1X + m_2Y + m_3Z = d$ in orthogonal space.

Plane I: rhodanine, II: methylpropenylidene, III: benzene, IV: carboxymethyl.

Plane	m_1	m_2	m_3	d
I	0.010 85	-0.876 13	0.481 95	1.581 95
II	-0.025 76	-0.919 02	0.393 36	0.977 36
III	0.102 75	-0.834 59	0.541 21	2.766 20
IV	0.268 92	0.423 82	0.864 90	4.434 53

(2) Deviations ($\times 10^3$, Å) from the best plane, with e.s.d.s in parentheses.

I	II	III	IV
N(2)* 6(5)	C(4)* 4(6)	C(10)* 26(7)	C(1)* 0(7)
C(3)* -14(6)	C(6)* -3(6)	C(11)* -36(7)	O(1)* -6(6)
S(4)* 1(2)	C(7)* -7(5)	C(11')* 7(7)	O(1')* 4(6)
C(4)* -9(6)	C(8)* 1(6)	C(12)* 13(7)	C(2)* 8(8)
C(5)* 3(6)	C(9)* 1(8)	C(12')* -39(7)	N(2) 10(11)
C(2) 21(7)	C(10)* 4(7)	C(13)* 30(8)	
S(3) -47(7)	S(4) -170(6)	C(8) -15(9)	
O(5) 5(6)	C(5) 62(8)		
C(6) -115(8)	C(11) 189(8)		
	C(11') -265(8)		

(3) Dihedral angle (°) between the best planes, with e.s.d.s in parentheses.

	II	III	IV
I	5.8(5)	6.7(2)	92.8(6)
II		12.0(5)	87.0(7)
III			98.2(6)

*Atoms with asterisks define the plane in each case.

acetone to avoid the effect of molecular self-aggregation. All NMR spectra were measured on a Varian VXR-200 or a VXR-500 (200 or 500 MHz for ^1H , respectively) spectrometer. The solvent deuterium resonance was used to lock the proton signals

of the sample. The chemical shifts were measured downfield from internal tetramethylsilane (TMS). In the nuclear Overhauser enhancement (NOE) experiments the decoupler was set to the first of four multiplets and 16 transients were recorded (quadrature detection). The decoupler was then moved to the next multiplet, and finally far off the resonance. Each multiplet was irradiated to saturate the signal. The quantitative NOE data were evaluated as follows: the normal and saturated spectra were simultaneously displayed on the screen and then subtracted. The difference spectrum was plotted and then the integration was performed. The intensity of the proton being saturated was used as the reference, and NOEs were measured with respect to this peak.

Results and Discussion

Molecular Dimension and Conformation.—A stereoscopic (ORTEP²⁴) drawing of epalrestat is shown in Figure 1. The bond lengths and angles between non-hydrogen atoms are given in Table 3. Selected torsion angles and the optimal planes with their dihedral angles are listed in Tables 4 and 5, respectively. The bond lengths and angles obtained show no noticeable abnormality, although their estimated standard deviations (e.s.d.s) are somewhat large because of the relatively high thermal motion of each atom. The lengths of C(6)–C(7) [1.416(7) Å] and C(8)–C(10) [1.469(7) Å] bonds are noticeably less than the normal C–C single-bond length (1.541 Å), and are in a partial double-bond region as a result of the resonance with neighbouring π -bonds. This effect leads the propenylidene bond sequence to result in a planar arrangement (Table 5); the torsion angles C(5)–C(4)–C(6)–C(7), C(4)–C(6)–C(7)–C(8), C(6)–C(7)–C(8)–C(10), and C(7)–C(8)–C(10)–C(11) are all in the *trans* region near to 180° (Table 4). This plane is almost coplanar with the rhodanine and benzene rings, and their dihedral angles are 5.8(5) and 12.0(5)°, respectively (Table 5). As a result of this extensive planarity of epalrestat (see Figure 1), the covalent bonding of the C(9) methyl group to C(7) causes enlargement of the C(9)–C(7)–C(8) [125.5(3)°] and C(8)–C(10)–C(11') [126.4(3)°] bond angles. The carboxyl group in which a hydrogen atom is covalently attached to O(1') is in a

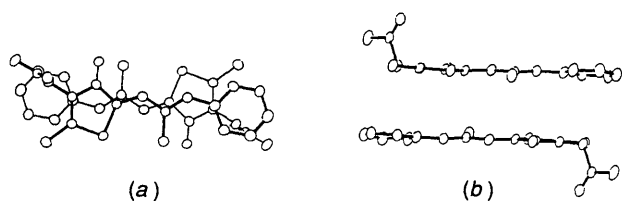


Figure 3. Overlapping of two centrosymmetrically related epalrestat molecules, viewed perpendicular (a) and parallel (b) to the planar plane.

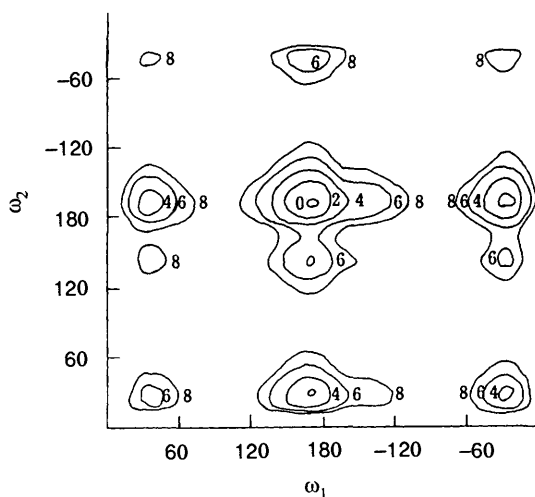


Figure 4. Contour map of (ω_1, ω_2) . The contour numbers represent the energy difference (in kcal mol^{-1}) from the most stable energy value (ω_1 170.0° , ω_2 -170.0°).

neutral form and is almost at right angles to the rhodamine ring; the dihedral angle between them is $92.8(6)^\circ$. This rectangular orientation of the carboxymethyl group directly attached to the heterocyclic ring could be energetically stable and has been most frequently observed in related compounds.²⁵

The chemical structure of epalrestat has been considered to be (*E*)-3-carboxymethyl-5-[(*2E*)-2-methyl-3-phenylpropenylidene]rhodanine,⁷ and epalrestat was used as a key compound for the investigation of the structure-activity relationship of ARIs.²⁶ However, the present X-ray crystal analysis clearly showed that the structure of epalrestat should be revised to (*Z*)-3-carboxymethyl-5-[(*2E*)-2-methyl-3-phenylpropenylidene]rhodanine. It is important to note that this compound, though stable in the dark, isomerizes very easily by photoirradiation even under a room light in solution to afford four isomers, including the (*E*)-isomer.²⁷

Crystal Packing and Molecular Interactions.—Crystal packing viewed along the *c*-axis is shown in Figure 2, where hydrogen atoms are omitted for clarity. Two epalrestat molecules in a unit cell, which are related by a centre of symmetry, are bonded to each other by van der Waals contacts and hydrogen bonds with ethanol solvents. No noticeable short contacts were observed in the crystal packing. Ethanol molecules, which locate in the cavities formed by the molecular packing of epalrestat, stabilize the crystal structure by hydrogen-bond formation [$\text{O}(1)\text{E} \cdots \text{O}(1')$ $2.592(6)$ Å] and short contacts [$\text{C}(3)\text{E} \cdots \text{O}(1')$ $3.39(2)$, $\text{C}(3)\text{E} \cdots \text{C}(2)$ $3.41(2)$, and $\text{C}(3)\text{E} \cdots \text{S}(3)$ $3.28(2)$ Å]. The presence of only one hydrogen bond between the ethanol and epalrestat molecules, and the relatively

Table 6. ^1H NOE data (%) of epalrestat in $[\text{D}_6]\text{acetone}$ solution.

Irradiation	Proton (NOE ^a)
6-H	8-H (22.7) 9-H (0.6)
8-H	6-H (26.9) 11- or 11'-H (3.6)
9-H	6-H (5.8) 11- or 11'-H (5.7)
11- or 11'-H	8-H (2.3) 9-H (1.8)

^a The value corresponds to the NOE per proton. The average error is 0.1%.

loose van der Waals contacts, are the reasons why the crystals are very fragile and why the solvent molecules of crystallization are so labile.

As a characteristic of the molecular interactions observed in the crystal packing, the formation of an extensive stacking pair is shown in Figure 3. Two epalrestat molecules, which are related by a centre of symmetry and are therefore parallel, are stacked with an average vertical spacing of 3.45 Å; the dihedral angle between the rhodanine and benzene rings is $6.7(2)^\circ$. This stacking could result from the planar conformation of epalrestat, and could be stabilized by the dipole-dipole coupling by the antiparallel alignment of the long axes of respective epalrestat molecules (3.251 D) and by electrostatic interactions; the electron-rich and -deficient atomic pairs are involved in the stacking, *i.e.*, $\text{N}(2)$ (0.0208 e) \cdots $\text{C}(10)$ (0.0133 e) 3.534 Å, $\text{S}(3)$ (-0.3387 e) \cdots $\text{C}(11)$ (0.0058 e) 3.913 Å, $\text{S}(4)$ (-0.0768 e) \cdots $\text{C}(8)$ (0.0077 e) 3.980 Å, $\text{C}(4)$ (-0.0518 e) \cdots $\text{C}(7)$ (0.0093 e) 3.544 Å, and $\text{O}(5)$ (-0.3921 e) \cdots $\text{C}(7)$ (0.0093 e) 3.795 Å.

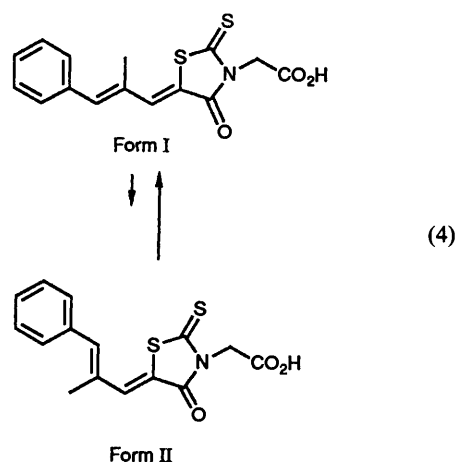
Conformational Energy Analysis of Epalrestat.—If the planar conformation observed in the crystal structure represents the energetically stable form of epalrestat itself, this would be important for considering the molecular modelling of potent ARIs. Since it is well known that a molecular conformation in the crystal state is highly likely to be affected by external forces such as crystal-packing forces, the conformational analysis of epalrestat was carried out by a molecular mechanics method. The contour energy map for (ω_1, ω_2) rotation is shown in Figure 4. As is obvious from this figure, the extended conformation (ω_1 160 – 180° , ω_2 -150 to -180°) is the most energetically stable, and has an energy value of -21.179 kcal mol^{-1} * at ω_1 170.0° , ω_2 -170.0° , which is 1.565 kcal mol^{-1} more stable than the second one (ω_1 -30.0° , ω_2 -170.0°). This result clearly shows that the planar conformation is the most stable form inherent in epalrestat, both crystallographically and theoretically.

Solution Conformation of Epalrestat.—In order to examine the molecular conformation of epalrestat in solution, NMR analysis in $[\text{D}_6]\text{acetone}$ solution was attempted. As was previously stated, structural isomerization of epalrestat at room temperature takes place easily. This makes it very difficult to use exact chemical shifts and coupling constants of protons for estimating its molecular conformation. On the other hand, the measurement of NOE which reflects the spatial proximity of pairs of protons in solution, provides accurate conformational information for a desired molecule, irrespective of the coexistence of isomers.

Exact NOEs were measured by 1D- ^1H NOE experiments, and the results are presented in Table 6. The most significant NOE was observed for 6-H upon irradiation of 8-H, and *vice versa*. This reflects the *cis* orientation between the C-6-6-H and

* 1 cal = 4.184 J.

C-8-8-H bonds. On the other hand, a slight, but detectable, NOE was measured between 6-H and 9-H, suggesting that these protons protrude to the same side of the molecular plane. Thus these NOE data show the existence of the following conformational equilibrium of epalrestat in solution [equation (4)].



With respect to the molecular conformation of Form II, an ω_1 value of $\pm 30^\circ$ is possible, judging from conformational energy calculations (Figure 4).

Conformational Characteristics of Epalrestat as a Potent ARI.—X-Ray crystallographic, energy calculational, and NMR solution studies suggested the planar conformation (Form I) of epalrestat as the most stable conformation; the conformation of Form II also exists as a minor form in solution. Since this compound is one of the most potent ARIs known⁷ (see Table 1), it is interesting to consider how this planar conformation relates to the emergence of AR inhibitory activity.

Previous studies on the mechanism of AR inhibition have shown that certain electrostatic and steric requirements are necessary for biological activity.^{3,28} Kador *et al.*^{26,28} have proposed a possible binding mode between AR and its inhibitor. According to this model, the binding pocket of the enzyme consists of two hydrophobic sites (H1 and H2) and a hydrogen-bonding or charge-transfer (CT) site, and their correct relative disposition is very important for tight binding with ARI to occur. By reference to (i) previous considerations on the structure-activity relation of oxazolecarbamate derivatives¹⁶ and (ii) conformational comparisons with other ARIs such as alconil, statil, and 4-isopropyl-BPOC (Table 1), a proposed binding mode of epalrestat to the H1, H2, and CT sites of AR is schematically illustrated in Figure 5, where the epalrestat can be considered to take either conformation Form I or Form II. The methylphenylpropenylidene and carboxymethylrhodanine moieties would correspond to the H1 and CT sites, respectively, and the structural moiety binding to the H2 site

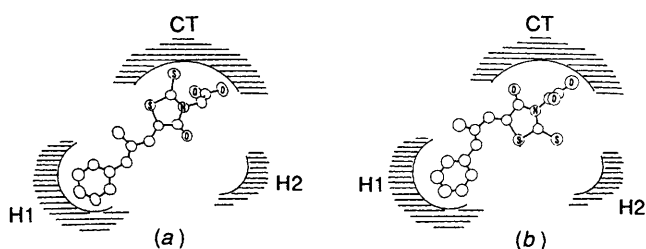


Figure 5. Schematic diagram of the proposed binding mode of epalrestat Form I (a) or Form II (b) with an AR enzyme. The conformation of Form II corresponds to $\omega_1 - 30^\circ$.

appears to be lacking in both conformations of the epalrestat. The distance between the central positions of the benzene and rhodanine rings is 7.62 Å for Form I and 6.80 Å for Form II; sorbinil, alrestatin, and tolrestat may also belong to this category, though a detailed QSAR analysis has not yet been published.

Provided that the binding mode proposed in Figure 5 is acceptable for the emergence of AR inhibitory activity, it could be supposed that the H2 site is not necessarily required for the activity, but, rather, enhances hydrophobic binding with the ARI. On the other hand, the interaction with the CT site is absolutely necessary for the activity, because 3-alkylrhodanines already show potent ARI activity.²⁸ The significant charge-transfer interaction between the rhodanine ring of epalrestat and the tyrosine residue²⁹ of AR, and multiple hydrogen-bond formation between the polar atoms of 3-carboxymethylrhodanine and the AR backbone and side-chains are, most probably, necessary for the tight binding of the ARI with CT site. The 2-methylphenylpropenylidene moiety may stabilize the interaction with AR by the usual van der Waals forces (H1 site).

The present study may help in delineating the pharmacophore requirements of ARIs. Based on the planar conformation of epalrestat, it may now be possible to extract the necessary common structural features from a wide variety of potential ARI substances.

References

- 1 K. H. Gabbay, *Annu. Rev. Med.*, 1975, **26**, 521.
- 2 P. F. Kador, Y. Akagi, and J. H. Kinoshita, *Metabolism*, 1986, **35** (Suppl. 1), 15.
- 3 P. F. Kador, W. G. Robinson, Jr., and J. H. Kinoshita, *Annu. Rev. Pharmacol. Toxicol.*, 1985, **25**, 691.
- 4 M. P. Cohen, 'The Polyol Paradigm and Complications of Diabetes,' Springer-Verlag, New York, 1987, p. 25.
- 5 J. H. Kinoshita, P. F. Kador, and M. Datiles, *J. Am. Med. Assoc.*, 1983, **246**, 257.
- 6 J. H. Kinoshita, *Invest. Ophthalmol.*, 1974, **13**, 713.
- 7 H. Terashima, K. Hama, R. Yamamoto, M. Tsuboshima, R. Kikkawa, I. Hatanaka, and Y. Shigeta, *J. Pharmacol. Exp. Ther.*, 1984, **229**, 226.
- 8 M. J. Peterson, R. Sarges, C. E. Aldinger, and D. P. MacDonald, *Metabolism*, 1979, **28** (Suppl. 1), 456.
- 9 B. M. York, *Eur. P. Appl. 0 092 385/1983* (*Chem. Abstr.*, 1984, **100**, 185790g).
- 10 K. H. Gabbay, N. Spack, S. Lod, H. J. Hirsh, and A. Ackil, *Metabolism*, 1979, **28** (Suppl. 1), 471.
- 11 K. Sestanj, F. Bellini, S. Fung, N. Abraham, A. T. L. Humber, N. Simard-Duquesne, and D. Dvornik, *J. Med. Chem.*, 1984, **27**, 256.
- 12 D. Stribling, D. J. Mirrless, H. E. Harrison, and D. C. N. Earl, *Metabolism*, 1985, **34**, 336.
- 13 T. Tanimoto, H. Fukuda, T. Yamaha, Y. Ohmomo, M. Nakao, and C. Tanaka, *Chem. Pharm. Bull.*, 1986, **34**, 2501.
- 14 J.-M. Rondeau, J.-P. Samama, B. Samama, P. Barth, D. Moras, and J.-F. Biellman, *J. Mol. Biol.*, 1987, **195**, 945.
- 15 F. K. Winkler, A. D'Arcy, and W. Pirson, *J. Mol. Biol.*, 1987, **197**, 763.
- 16 T. Ishida, Y. In, H. Ohishi, D. Yamamoto, M. Inoue, C. Tanaka, Y. Ueno, Y. Ohmomo, N. Kanda, A. Tanaka, and T. Tanimoto, *Mol. Pharmacol.*, 1988, **34**, 377.
- 17 E. H. Fischer and H. Hibbert, *J. Am. Chem. Soc.*, 1947, **69**, 1208.
- 18 P. Main, S. E. Hull, L. Lessinger, G. Germain, J. P. Declercq, and M. M. Woolfson, MULTAN78. A System of Computer Programs for the Automatic Solution of Crystal Structures from X-Ray Diffraction Data, Universities of York and Louvain, Belgium, 1978.
- 19 The Universal Crystallographic Computing System—Osaka, The Computation Center, Osaka University, Osaka, Japan, 1979.
- 20 D. T. Cromer and T. Waber, in 'International Tables for X-Ray Crystallography,' eds. J. A. Ibers and W. C. Hamilton, Kynoch Press, Birmingham, 1974, vol. 4, p. 71.
- 21 Molecular Design, Ltd., CHEMLAB-II. A Molecular Modeling Software System, San Leandro, CA, 1986.
- 22 M. J. S. Dewar and W. J. Thiel, *J. Am. Chem. Soc.*, 1977, **99**, 4899.

- 23 A. J. Hopfinger and R. A. Pearlstein, *J. Comput. Chem.*, 1984, **5**, 486.
- 24 C. K. Johnson, ORTEP-II: A Fortran Thermal-Ellipsoid Plot Program for Crystal Structure Illustrations, ORNL-5138, Oak Ridge National Laboratory, 1976.
- 25 M. Inoue, Y. Okuda, T. Ishida, and M. Nakagaki, *Arch. Biochem. Biophys.*, 1983, **227**, 52.
- 26 P. F. Kador, J. H. Kinoshita, and N. E. Sharpless, *J. Med. Chem.*, 1985, **28**, 841.
- 27 T. Ishida, Y. In, M. Inoue, Y. Ueno, C. Tanaka, and N. Hamanaka, *Tetrahedron Lett.*, 1989, **30**, 959.
- 28 U.S.P. 4 464 382/1984, E.P.C.P. 0 047 109/1981.
- 29 P. F. Kador and N. E. Sharpless, *Mol. Pharmacol.*, 1983, **24**, 521.

Paper 9/05139B

Received 1st December 1989

Accepted 1st February 1990